Infrared Thermal Image Profiling for Gearless Hoisting Motor Condition Monitoring

Jonathan Benedict M. Gonzales[1], Carlos Anthony B. Petilla[2], Patrick Laurence L. Yuson[3], Macario II O. Cordel[4], and Emmanuel A. Gonzalez[5]

College of Computer Studies, De La Salle University – Manila
[1] Department of Computer Technology, jonathan_benedict_gonzales@dlsu.ph
[2] Department of Computer Technology, carlos_petilla@dlsu.ph
[3] Department of Computer Technology, patrick_yuson@dlsu.ph
[4]Department of Computer Studies, mac.cordel@delasalle.ph
[5]Jardine Schindler Elevator Corporation, 8/F Pacific Star Bldg.,
Sen. Gil Puyat Ave. cor. Makati Ave., Makati City 1209, Philippines
emm.gonzalez@delasalle.ph

Abstract: Technology nowadays has provided different industries more efficient machinery and tools in order to improve their products and services, wherein time and other resources are needed in order to maintain them in proper condition. An example would be the machines used to operate elevators, wherein excessive strain is applied on its components, especially on the motor. In order to mitigate any major faults, condition-based monitoring is performed on the motor through various means; one of which is thermographic monitoring. Thermographic monitoring is the inspection of thermal patterns on an object's surface and assessing whether it has any irregularities in temperature in any part of it. Since there is no available objective basis of a regular and irregular thermal image of a lift system motor, it is not possible to assess the actual condition of a motor. This study then aims to create a system in analyzing thermal images of, specifically, gearless lift system motors. First, the system defines and extracts regions of interests (ROIs) that pertain to significant portions of the actual motor. Second, each ROI is then segmented into equally-sized cells/segments for relatively consistent temperature profiling, which deals with averaging pixel values, noting that certain ranges of pixel values pertain to certain ranges of temperatures. Lastly, the temperature profiles are then retrieved and tabulated accordingly by each segment, placing it in a predefined dictionary of temperature profiles. Initial profiles are then continuously integrated with new input temperatures from newly processed thermal images, if within tolerance value. This then entails the establishment of an objective ground basis of a regular-condition motor's thermal outlook. In conclusion, the results show that the computations are 99.9% accurate in comparison to the data shown in the thermography software application used. This ground basis can then be utilized in creating further intelligent systems in relation.

Key Words: condition-based maintenance; thermographic monitoring; temperature profiling

1. INTRODUCTION

Various industries nowadays use intricate technologies in order to meet further optimization in their respective trades. But in line with doing so, these industries also need to consider appropriate maintenance methods. This is because these complex equipment and tools tend to deteriorate in efficiency and overall functionality over the course of time of their usage. Generally, maintenance is required to have efficient and productive operations and also to maximize waste reduction, wherein its cost is significantly smaller than the cost in consequence of a major breakdown (Krar, n.d.).

Such is also the case in the lift system (or elevator) industries. Lift systems composed of electromechanical components deteriorate over time and is not visible to the naked eyeF. Condition-based maintenance is then mostly performed on a lift system due to the critical risk of it causing fatal consequences upon the lift system and, ultimately, its passengers. One method for condition-based maintenance is through capturing and analyzing thermal signatures of a lift system's motor in order to assess whether there are irregularities in its thermal distribution. This approach is similar to the risk-based inspection study widely discussed in the paper “An implementation of risk-based inspection for elevator maintenance” by Park and Yang (2010).

2. OBJECTIVES, SCOPE, AND LIMITATIONS OF THE STUDY

Thermal images of the motors are produced during previous maintenances, wherein most of the time, due to previous condition-based and preventive maintenances, they are of regular conditions. This then limits the source of an objective basis of what a normal or defective motor's thermal signature should look like. This eventually results to the reliance on the assessments of specialists to know which is which, which are then entirely subject to human error. This gives rise to the need of an intelligent system to properly assess these thermal images and significantly decrease any margin of error. But before doing so, a system for producing initial data to serve as ground basis of comparison for the utilization of further intelligent systems should first be created.

The main objective then of this study is to develop a system in analyzing thermal images of gearless lift system motors based on color distribution, and computing for the average temperature ranges within each thermal image.

The thermal images used are of the motors of the *Schindler PMS420 synchronous motor* elevator model, and are acquired through the use of an *Acez BG1600/3200* infrared thermograph. The process that the system performs is limited to analyzing only monochromatic images.

3. METHODOLOGY

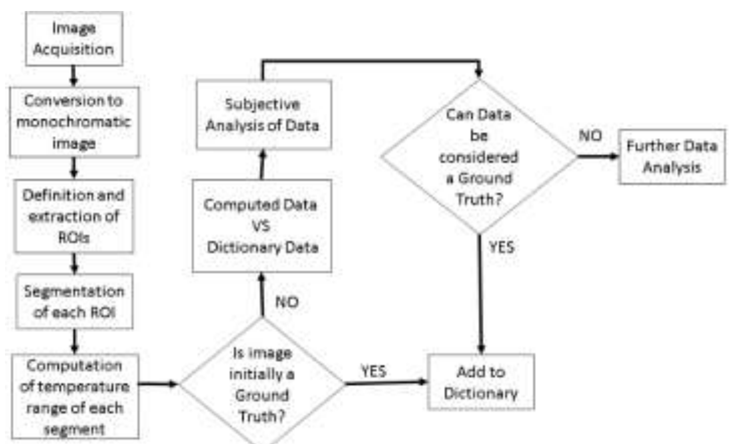

Fig. 3.1. Block Diagram of the System

First, the thermal images were acquired through an infrared thermograph (IRT). These images are initially produced in monochrome through the IRT’s default settings but are visually modified into various color palettes, such as *High Contrast*, *Hot Metal*, and *Isotherm Style*, available in the IRT’s accompanied software application, *ACEZ BG Analysis*. An image’s color palette is then set to *White Hot Mono* since it closely resembles a monochromatic outlook of the image and it has a relatively efficient sample distribution based on its generated histogram, as shown below:

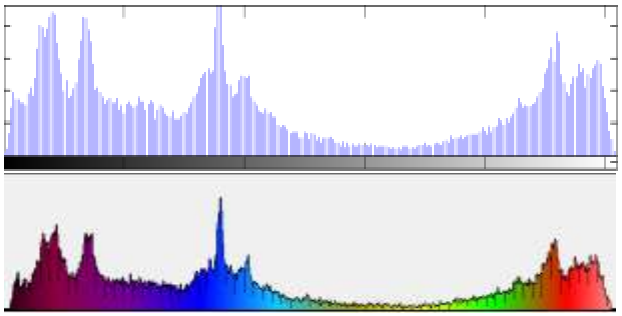

Fig.3.2. Sample Distribution of the Monochromatic Image (above) vs the Actual Sample Distribution (below)

The thermal image was input into the system, wherein the system defined the three (3) ROIs in the motor image and extracted each of them. Each ROI is then segmented into predefined dimensions of cells/segments (e.g. ROI 1 – 9 cells long and 6 cells wide). Each segment is then traversed to compute for the minimum and maximum temperature ranges within it, wherein there is an underlying conversion of pixel values into temperature values. After computing for the values, the results are then compared with the current base values in the predefined dictionary of values obtained from previously processed thermal images. If values are within tolerance range, the averaged values are then integrated into the dictionary. Otherwise, the images are disregarded from the system and are reconsidered for subjective analysis.

4. REGIONS OF INTEREST (ROIs)

4.1. Definition of ROIs

As shown in Figure 4.1, there are, essentially, three (3) ROIs in a particular thermal image of a gearless lift system motor. The ROIs were specified base on the components located in that particular area. The stator of the motor I located at Region 1, and the two exhaust fans are located at Region 3.

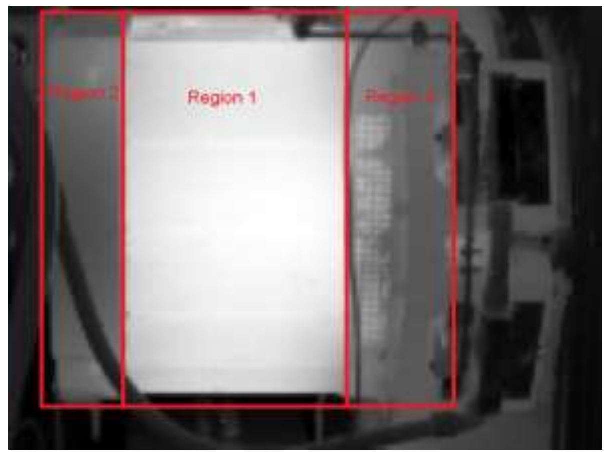

Fig. 4.1. Regions of Interest of Thermal Image

These ROIs are outlined by the system by first computing the grayscale threshold (using *grayscale* function in MATLAB), and then removing all gray colors below the computed threshold (using *im2bw* function in MATLAB). Examples of defined ROIs are shown in Figures 4.2, 4.3, and 4.4.

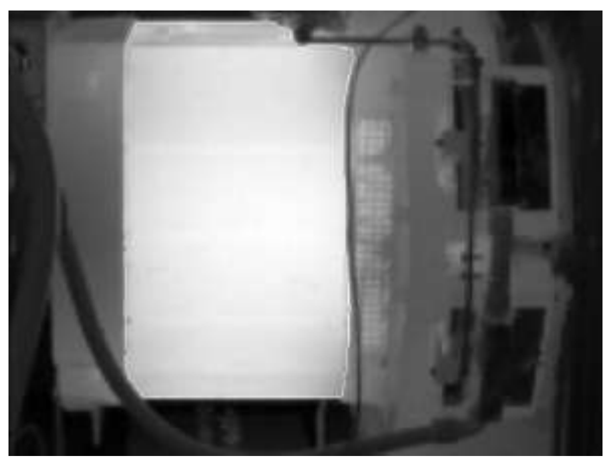

Fig. 4.2. ROI 1 – Center portion is outlined by a white line

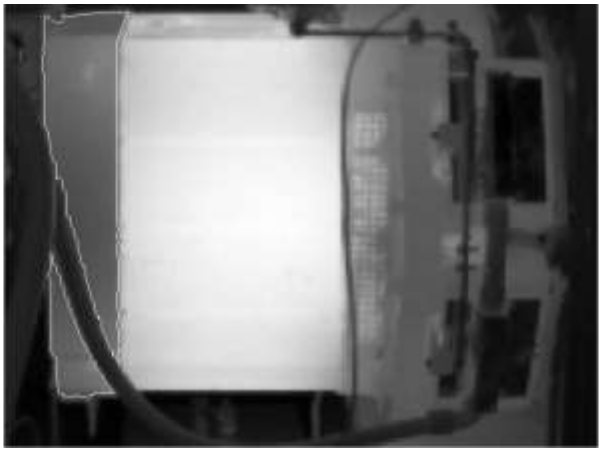

Fig. 4.3. ROI 2 – Left portion is outlined by a white line

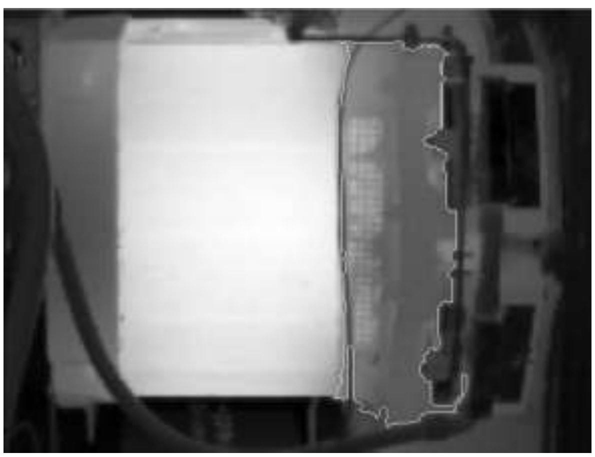

Fig. 4.4. ROI 3 – Right portion is outlined by a white line

4.2. Extraction and Segmentation of ROIs

Each defined ROI is extracted and dealt with separately. The extracted ROI is then segmented into discrete dimensions of equally-sized cells/segments. The dimensions (length by width) of ROI 1, 2, and 3 are 6x9 cells, 2x9, and 3x9, respectively. This allows dynamic adjustment of the cells' sizes based on the overall size of the entire motor in the image. Also, it allows relative consistency in the values to be computed in each cell. Examples of segmented ROIs are shown in Figures 4.5, 4.6, and 4.7.

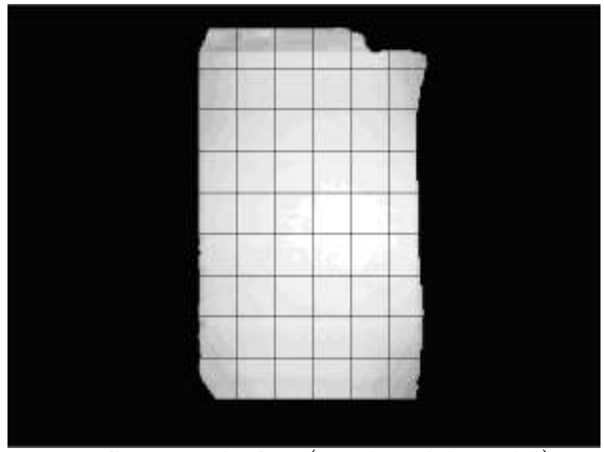

Fig. 4.5. Segmented ROI 1 (6x9; length by width)

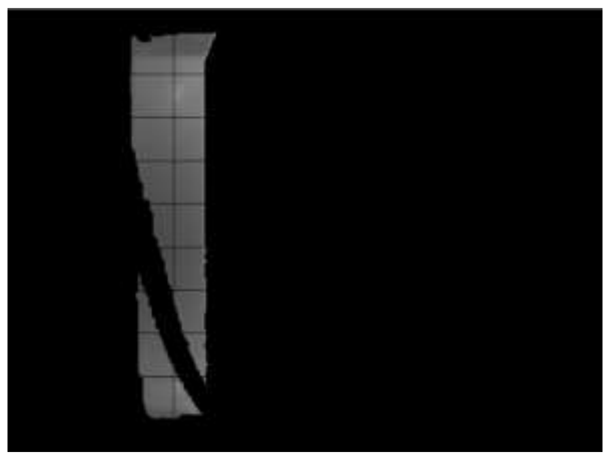

Fig. 4.6. Segmented ROI 2 (2x9; length by width)

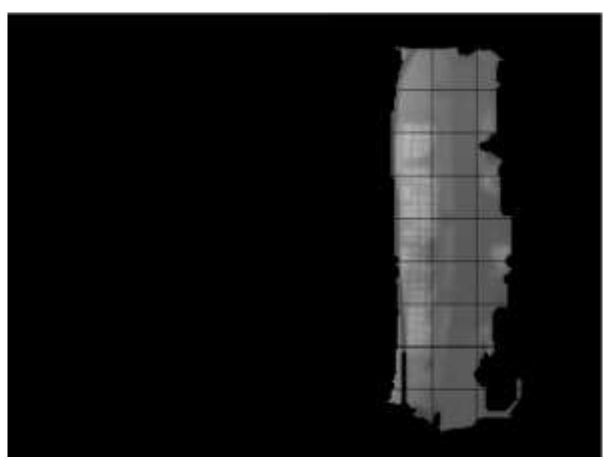

Fig. 4.7. Segmented ROI 3 (3x9; length by width)

5. TEMPERATURE PROFILING

5.1. Pixel-Temperature Conversion

After segmentation of each ROI, the average temperature values of each cell are then computed. Preceding this, pixel values are first converted to temperature values by spanning the lower and higher boundary of temperature values of a certain thermal image and correlating the pixel value, as shown in the following equation:

$$Temperature = \frac{P \times (Bu - Bl)}{255} + Bl \qquad \text{(Eq. 1)}$$

where:

P = pixel value
Bu = upper boundary *(°C)*
Bl = lower boundary *(°C)*

Using this equation, the temperature yielded is used in representation of each pixel value obtained through traversal of an entire cell's area. The temperatures obtained are a value range of the minimum and maximum temperatures within a certain cell. Boundaries can be obtained from the specified thermograph's settings.

5.2. Tolerance Value

The system then assesses whether a certain thermal image is within tolerance value of a certain cell. It is done to attain a consistent profiling of only normal-condition gearless lift system motors. If ever a cell within any ROI of a certain image is way off from the tolerance value, the image is then disregarded. Tolerance value is obtained by dividing the standard deviation of temperature values by the average of existing temperature values in the predefined dictionary, as shown below:

$$Tolerance = \frac{Standard\ Dev.\ of\ Temp.\ Values}{Average\ of\ Temp.\ Values} \qquad \text{(Eq. 2)}$$

5.3. Integration of Dictionary

If ever the averaged value range of a cell is within tolerance, the results are then integrated in a predefined dictionary of the results of previously processed thermal images, thus updating the base values of the minimum and maximum temperatures for each cell of each region.

6. System Analysis

6.1. Pixel-Temperature Conversion Analysis

Shown in the following tables are the results of several sample processed images, each of which shows the comparison of the computed and actual temperature ranges for segments 1-6 of ROI 1 given with the specified temperature boundaries:

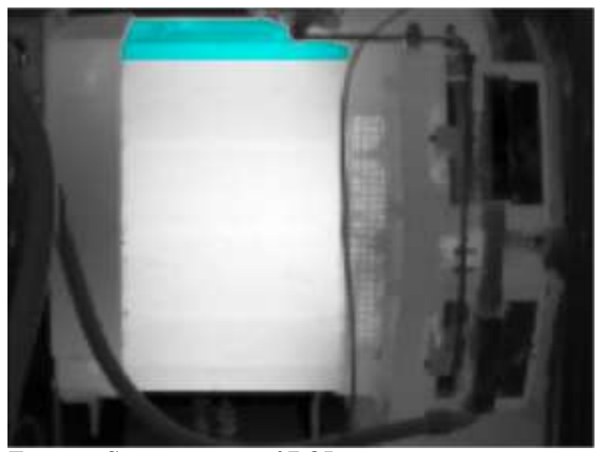

Fig. 4.8. Segments 1-6 of ROI 1

Table 5.1. Sample Image 1 (27.8 – 58.4)

Segment	Computed Min (°C)	Actual Min (°C)	Computed Max (°C)	Actual Max (°C)
1	45.32	45.3	53.12	53.1
2	47.72	47.7	54.92	54.9
3	48.44	48.4	55.76	55.7
4	46.76	46.7	55.64	55.6
5	46.64	46.6	55.4	55.4
6	44.84	44.8	53.12	53.1

Table 5.2. Sample Image 2 (27.6 – 58.8)

Segment	Computed Min (°C)	Actual Min (°C)	Computed Max (°C)	Actual Max (°C)

1	43.99	43.9	53.41	53.4
2	48.64	48.6	55.37	55.3
3	47.42	47.4	56.35	56.3
4	47.29	47.2	56.23	56.2
5	44.48	44.4	56.1	56.1
6	44.11	44.1	53.9	53.9

Table 5.3. Sample Image 3 (27.9 – 58.9)

Segment	Computed Min (°C)	Actual Min (°C)	Computed Max (°C)	Actual Max (°C)
1	44.0	44.0	53.42	53.4
2	47.59	47.5	55.61	55.6
3	49.66	49.6	56.22	56.2
4	46.74	46.7	56.35	56.3
5	44.55	44.5	56.10	56.1
6	44.31	44.3	53.67	53.6

Table 5.4. Sample Image 4 (39.7 – 63.5)

Segment	Computed Min (°C)	Actual Min (°C)	Computed Max (°C)	Actual Max (°C)
1	51.92	51.9	56.22	56.2
2	52.20	52.2	57.9	57.9
3	52.58	52.5	58.74	58.7
4	52.58	52.5	60.79	60.7
5	53.23	53.2	58.08	58.0
6	52.39	52.3	54.72	54.7

Results yield a 99.9% accuracy for temperature reading of segments 1-6 of ROI1 on four (4) different thermal images.

6.2. Dictionary Data Analysis

Given two (2) new images where Image 1 is considered normal at operating condition and Image 2 as an unanalysed image for analysis of segment 1 of ROI1, shown in the next set of tables are the temperature range values computed by the system and the average temperature values from the dictionary.

Table 5.5. New Image 1 (28.0 – 52.2)

	Image data (°C)	Dictionary Data (°C)
Max	49.54	52.25
Min	42.70	45.51

For segment 1 of ROI 1, New Image 1 has a computed temperature range of 42.7°C to 49.54°C whereas the average temperature range for normal operating condition ranges from 45.51°C to 52.25°C. Since Image 1 has been predefined to contain values of normal temperature ranges, associated computed values can be added to the dictionary for broader temperature range analysis.

Table 5.6. New Image 2 (28.1 – 52.2) with updated Dictionary Values.

	Image data (°C)	Dictionary Data (°C)
Max	49.83	52.06
Min	43.50	45.31

Table 5.6 shows the computed temperature range of New Image 2 in segment 1 of ROI1 with an updated set of dictionary values, where the normal average temperature range is now 45.31°C to 52.06°C from the older 45.51°C to 52.25°C. These temperature values cannot be directly interpreted as New Image 2 with a min temperature value of 43.50°C is only off by 1.81°C which can be considered as normal under operating condition, the tolerance value of the dictionary values must be considered.

6.3. Tolerance Conversion Analysis

Table 5.7. New Image 2 (28.1 – 52.2) with computed Tolerance percentage

	Image data (°C)	Dictionary Data (°C)	Tolerance Value (%)

Max	49.83	52.06	5.11%
Min	43.50	45.31	6.33%

From the updated set of dictionary values, the computed tolerance value for segment 1 of ROI 1 is at 5.11% for max temperature values and 6.33% for Min temperature values. The average max temperature value now ranges from 49.4°C to 54.72°C and the average min temperature values now ranges from 42.45°C to 48.17°C. With these set of temperature ranges, the computed max and min temperature range for New Image 2 can be considered normal under operating conditions.

7. CONCLUSION

Based on the results, the system achieved 99.9% accuracy in its temperature reading for monochromatic thermal images. These data can then be integrated into the predefined dictionary, therefore establishing a broader and more reliable ground basis for the analysis of regular-condition gearless lift system motors. This can be utilized for further intelligent systems in assessing these types of motors as normal or defective in general.

8. REFERENCES

Krar, S. (n.d.). The Importance of Maintenance. Retrieved November 20, 2013, from http://www.automationmag.com/images/stories/LWTech-files/94%20Intelligent%20Systems.pdf

Park, S., Yang, B. (2010). An implementation of risk-based inspection for elevator maintenance [Electronic version]. Journal of Mechanical Science and Technology, 24, 2367-2376